IEEE Transactions on Nuclear Science, Vol. NS-30, No. 4, August 1983

THE ADVANCED TEST ACCELERATOR (ATA) INJECTOR*

C. H. Jackson, D. G. Bubp, T. J. Fessenden, R. E. Hester
V. K. Neil, A. C. Paul+ and D. S. Prono

Lawrence Livermore National Laboratory
P. O. Box 808, L-436
Livermore, California 94550

SUMMARY

The ATA injector, developed from experience gained from the Experimental Test Accelerator (ETA) linac, has recently been completed. The injector consists of ten 0.25 MV cells that are used to develop 2.5 MV across a single diode gap. The 10 kA beam is extracted from a 500 cm^2 plasma cathode at average rates of up to 5 Hz and burst rates to 1 kHz. Pulsed power from 20 water filled blumleins is divided and introduced symmetrically through four ports on each cell. All major insulators are fabricated from filled epoxy castings. With these improvements, the ATA injector is smaller than the ETA injector; has a faster pulse response; has lower voltage stress on insulators and higher ultimate performance. Injector characterization tests began in October, 1982. These tests include beam current, energy, and emittance measurements.

INTRODUCTION

During the initial planning of the ATA Program, it was established that the ETA injector[1] would be utilized for this second generation machine. However, by late 1980 the valuable stream of Physics data and engineering experience coming from operation of the ETA made the thought of termination untenable. It was determined that a new injector would be cost effective since it would permit incorporation of recent experience gained in operation of ETA and it would also preserve the ETA as a test bed for further accelerator technology development.

Testing of the new injector started in October, 1982, just fifteen months after initiation of design. On the fifth day of testing, it met full design parameters; 10 kA, 2.5 MeV, 60 ns (Full Width Half Maximum).

DESIGN OBJECTIVES

Simply stated, we desired to improve performance, reliability and maintainability over that of the ETA. The realization of those objectives involved technical compromise, and value judgements were therefore weighted in the above order. Of the many objectives, ten are identified below.

1. Reduce the HV pulse rise/fall time.
2. Improve the flatness of the beam pulse.
3. Increase the output voltage capability.
4. Improve the accuracy and ease of machine alignment.
5. Reduce the overall size of the machine.
6. Improve coil cooling systems.
7. Modularize the structure, if possible.
8. Simplify material handling and assembly procedures to minimize down time.
9. Improve the vacuum pumping system.
10. Improved pulse power system[2].

*LLNL is operated by the Univ. of CA for the DOE, W-7405-ENG-48. This work is performed for the Dept. of Defense under DARPA (DOD), ARPA Order No. 4395, monitored by NSWC.

+Lawrence Berkeley Laboratory, Berkeley, CA 94720

INJECTOR CONSTRUCTION

Induction Cells

As can be seen from Fig. 1, the major departure from ETA is in the configuration of the accelerating voltage cells. The new cell configuration is similar to that used in the ETA Accelerator and provides the basis for several improvements:

1. Each cell now contains a separate oil/vacuum interface insulator. This change provides complete cell modularity for ease of repair and also reduces gap capacitance by 50%.
2. The addition of two more pulse power input ports per cell provides a reduction in input inductance and permits symmetrical power input from the dual blumlein source.
3. The accelerating gap is increased by .5" to 1.5", thus further reducing the gap capacitance as well as improving voltage holding capability.
4. The oil/vacuum interface insulator is fabricated from an alumina Trihydrate filled epoxy resin developed specifically for this purpose. The material is highly arc track resistant and provides a resistance to impact loading far superior to the ceramic which it replaces. Due to the size (52" diameter) and tolerances (± .010") required on this part, sizable cost savings were realized through the use of this material.

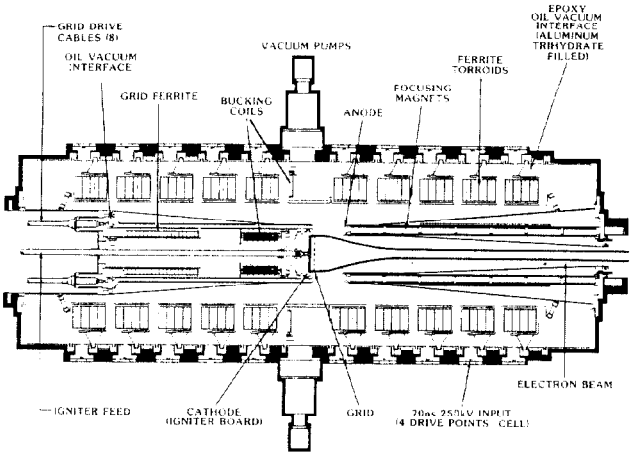

ATA 2.5MeV ELECTRON INJECTOR

Fig. 1

Anode Structure

The new anode has been improved with respect to both alignment precision and reliability. These improvements have been realized through the following changes:

1. The double cantilever construction is now "closed loop" for added structural rigidity.
2. Focus coils are prealigned on a precision mounting tube. The coil-tube subassembly is then located within the housing on a machined taper. Coil concentricity is thus maintained within ± .015".

0018-9499/83/0800-2725$01.00©1983 IEEE

3. Focus coils are directly cooled by tranformer oil flowing coaxially in the oil filled anode. At full coil power, exit oil temperature rise is only 31°F. The flooded anode design eliminates troublesome internal plumbing and also provides cooling to the beam tube, anode nose, steering coils and coil input connectors.

Cathode Structure

Significant improvements in the plasma cathode assembly have been realized through incorporation of some new features and a general reduction in mechanical complexity. The most significant changes from the ETA design and their virtures are identified as follows:

1. The cathode mounting structure provides for linear and angular movement in all three axes. Since these adjustments are all external, cathode alignment may be corrected without breaking vacuum.
2. The ignitor input insulator/vacuum barrier has been moved to a position immediately behind the cathode. This change reduces the total volume under vacuum and eliminates the need for a cathode vacuum pump. Additionally, the bucking coil and the igniter feed are now in air, greatly simplying the structure.
3. The grid drive connectors are replaced by a 300 kV design which was developed on the ETA.
4. The cathode B-field is now generated by two separately controlled bucking coils, one of which is located in the center pump station. This change allows the B_z component of the magnetic field to be reduced to approximately 0.1 G through the cathode.
5. The cathode is fitted with four precision hall sensors which provide a system for magnetically checking B-field alignment.

Vacuum System

The vacuum system consists of a central pump box with eight 6" diameter ports located radially about the accelerating gap. The vessel is terminated with a pump box at each end with two additional 6" ports in each. This provides for ten 6" cryopumps, a turbopump and a roughing line. Six cryopumps and a turbopump are presently fitted. With fifty-three square feet of epoxy insulator exposed to the vacuum, this system will maintain 5×10^{-6} Torr.

Alignment

Injector alignment is a three-level process. The anode and cathode magnets are aligned at the subassembly level to establish concentricity with the Z axis. First the anode is installed in the injector and the entire vessel moved as required to put the anode on beam line. The cathode is then installed and using the six degrees of freedom available in the cathode mounting structure, brought onto beam line. These procedures are implemented optically using internal targets and a line of sight along the beam line. The position of the cathode nose relative to the housing is then recorded using a pair of O-ring sealed X-Y probes located near the center pump station. These data are then used to verify cathode location after the internal targets have been removed and the cathode reinstalled. The vessel is fitted with four external targets and two clinometer flats on an auxiliary line of sight parallel to the beam line. These data, along with the X-Y probe data, permit verification of alignment after the injector has been pumped down and is in operational status. An additional check of B-fieldalignment is afforded by the hall sensors located in a plane 16 cm behind the cathode.

Material Handling

After reflecting on ETA experience, the problem of material handling was given high priority. With modularization of the induction cells assured, it was now possible to break the machine into fifteen relatively independent subassemblies, each weighing under 2500 pounds. A two-ton monorail is used to pluck individual subassemblies up and over the assembly to a dolly at the end of the curved rail system. The anode and cathode are handled in similar manner using a cantilever handling fixture. Two men can easily remove and replace any portion of the machine.

Beam Dynamics

Particle dynamics in the ATA gun are quite similar to those in the ETA gun. The capability of 3 MV anode voltage V_a rather than 2.5 MV in the ETA gun allows operation at 10 kA with a comfortable margin below the critical current for formation of a virtual cathode in the gun. The critical current is almost linear with anode voltage in these guns. Simulation predicts that the critical current is greater than 16 kA at 3 MV.

Downstream from the gun the beam current must be less than the space-charge limited current, I_ℓ, which is given approximately by the relation

$$I_\ell(kA) = \frac{17\,(\gamma^{2/3} - 1)^{3/2}}{1 + 2\ell\, n\,(b/a)} \qquad (1)$$

in which a is the beam radius, b is the radius of the surrounding beam pipe, and $\gamma = 1 + (eV_a/mc^2)$. The beam radius is determined by the solenoidal magnetic guide field B and a high value of B is desirable in order to suppress the beam breakup instability in the accelerator. The beam radius decreases with increasing magnetic guide field, but according to Eq. (1) the higher anode voltage of 3 MV allows for a smaller beam radius and a higher value of B in the transport downstream from the gun.

The beam emittance predicted by the simulation code EBQ is about the same for both guns, namely a normalized value of 0.3 to 0.4 rad-cm. This prediction is consistent with measurements of the beam emittance from both guns.

Experimental Results

Initial operation of the electron gun verified the successful implementation of the engineering improvements. Design parameters were rapidly achieved. The improved reliability of the pulsed power systems and the improved voltage holding capability of the electron gun were immediately apparent. Figure 2 shows HV waveforms and a beam current monitor at the 2.5 MeV operating level. The waveforms are very reproducible. The gun has operated as high as 3 MeV with great reliability.

Beam Emittance Measurements

The ATA beam emittance at the injector output was measured by the technique shown schematically in Fig. 3. The beam is allowed to impinge on a range thick carbon mask at a typical radius of 5 cm. The mask contains approximately 250 vertical and horizontal slots which divide the primary beam into a corresponding number of beamlets. The beamlets pass through a drift region of approximately 23 cm in which they freely expand. They then pass through a

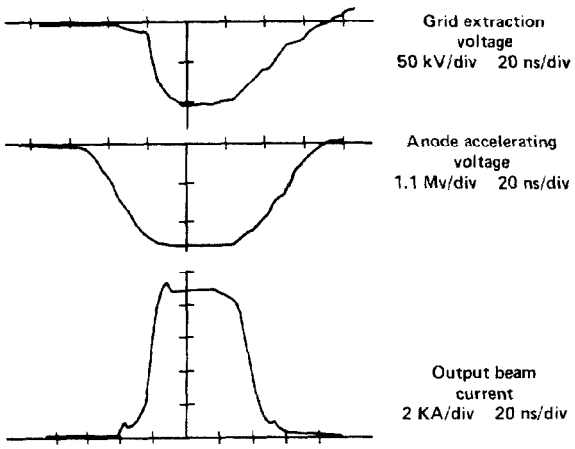

Fig. 2.

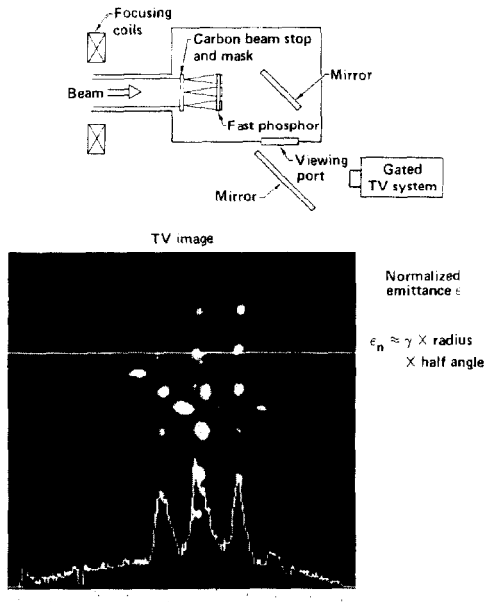

Fig. 3 Schematic and typical image scan from the ATA emittance box.

range thin aluminum foil and excite a fast phosphor deposited on the foil back. Using front surface mirrors the image created by the beamlets is relayed to a gated TV/computer system which records and analyzes the image. Four holes in the aluminum foil located symmetrically on a 3 cm radius circle about a center hole are used to calibrate the TV image.

The TV uses a micro-channel-plate intensifier in front of a charge-coupled silicon chip as the optical detector. The TV is capable of obtaining a picture in approximately 3.5 ns. In these experiments a 10 ns gate pulse was used. The TV image is "grabbed" electronically and digitized for storage and analysis by a microprocessor.

The computer obtains the emittance in the following way: The digitized TV image is normalized so that the brightest pixel has a value of 255. Then the calibration marks on the phosphor are used to inform the computer of the scale size of the TV image. Next the computer estimates the beam size by finding the rectangular area containing pixels of value greater than 128. The internal beam divergence is obtained by measuring the FWHM of the image sizes of the beamlets generated by the mask and dividing by the drift distance. For the experimental conditions of these measurements, the ATA beam was essentially at a waist.

Figure 4 shows normalized emittance measurements of the ATA beam at an energy of 2.5 MeV at currents varying between 6.5 and 10 kA. Each point represents from 20 to 40 individual emittance measurements. Shown are the mean of the data and one standard deviation.

Although the beam current measured in front of the emittance box was very reproducible, these measurements were troubled by a lack of reproducibility on a microscopic basis. Figure 3 shows that the beam is not uniform and the beam microstructure was repeatable on a pulse-to-pulse basis in only a general sense. For this reason the more detailed and precise reduction of the data that would yield a true phase plane plot of the beam was not possible. Nonetheless, the value of emittance obtained in these experiments is quite close to that anticipated from theory. Theory predicts that the fields near the grid should generate a normalized emittance near 0.3 rad-cm at beam currents considerably below the virtual cathode current limit. As the current approaches this limit, the emittance fluctuates then increases rapidly to very large values as the limit is reached. The data of Fig. 4 supports this dependence although the large statistical errors preclude quantitative conclusions.

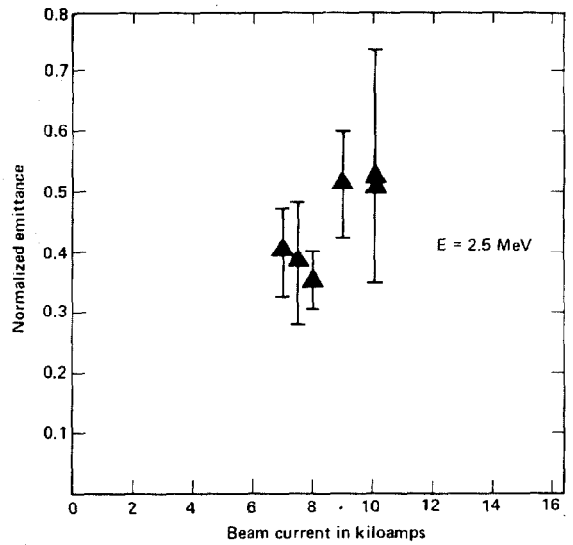

Fig. 4. Determinations of the emittance of the beam produced by the ATA injector. Each point represents approximately 25 measurements.

References

1. R. E. Hester, et. al., IEEE Trans. N. S. 26, 4180, (1979).
2. L. Reginato, Paper N2, this conference.